ELSEVIER

Ceramics International 33 (2007) 863–867

CERAMICS INTERNATIONAL

www.elsevier.com/locate/ceramint

Crystallization behaviour of Li_2O–ZnO–SiO_2 glass–ceramics system

Madhumita Goswami [a], P. Sengupta [b], Kuldeep Sharma [a], Rakesh Kumar [a], V.K. Shrikhande [a], J.M.F. Ferreira [c], G.P. Kothiyal [a,*]

[a] *Technical Physics and Prototype Engineering Division, Bhabha Atomic Research Centre, Mumbai 400085, India*
[b] *Materials Science Division, Bhabha Atomic Research Centre, Mumbai 400085, India*
[c] *Department of Ceramics and Glass Engineering, CICECO, University of Aveiro, Aveiro 3810-193, Portugal*

Received 11 November 2005; received in revised form 17 November 2005; accepted 2 January 2006
Available online 18 April 2006

Abstract

We have studied the crystallization behaviour in two types of lithium zinc silicate (LZS) glasses: (a) LZSL composition (wt.%): Li_2O, 12.65; ZnO, 1.85; SiO_2, 74.4; Al_2O_3, 3.8; K_2O, 2.95; P_2O_5, 3.15; B_2O_3, 1.2 (low ZnO); and (b) LZSH composition (wt.%): Li_2O, 8.9; ZnO, 24.03; SiO_2, 53.7; Na_2O, 5.42; P_2O_5, 2.95; B_2O_3, 5 (high ZnO). The glass has been prepared by usual melt–quenched technique. The crystallization was carried out following two different procedures: (i) cooling schedule (CS) and (ii) heating schedule (HS). The nucleation and crystallization temperatures were determined by DTA studies. In case of LZSL sample, the crystallization was carried out in the temperature range of 580–780 °C, whereas in case of LZSH it was done in the temperature range of 570 and 720 °C. Crystalline phases were identified using powder X-ray diffraction technique. Significant differences in the formation of crystalline phases and their relative ratios were observed between heating and cooling schedules. For LZSL, formation of Li_2SiO_3 phase along with small fraction of cristobalite phase was seen when CS was followed. On the other hand, mixed phase having small fraction of lithium zinc silicate in major cristobalite phase was obtained for heating schedule. However, in the case of LZSH, formation of lithium zinc silicate as major crystalline phase along with cristobalite phase is seen when HS was followed. For LZSL, the average thermal expansion coefficient (TEC) values were found to be around 178×10^{-7} and 114×10^{-7} °C^{-1}, for CS and HS, respectively, and for LZSH, TEC was found out to be $\approx 185 \times 10^{-7}$ °C^{-1} for HS. LZS glass–ceramics-to-Cu as well as to-SS-321 seals withstanding a vacuum of 10^{-6} Torr with leak rate 10^{-9} Torr l/s were fabricated using both compositions. Glass–ceramics-to-metal interface was studied using electron probe micro analysis (EPMA) to understand the mechanism of sealing.

Keywords: D. Glass ceramics; Thermal expansion coefficient; Microstructure; Lithium zinc silicate; Glass–ceramics-to-metal seal

1. Introduction

Glass–ceramics find various applications in the field of vacuum, sealing, electronics, cook wares, biomedical, etc. because of their superior thermal, mechanical, electrical and other physical properties compared to their parent glasses. In the process of conversion of glass to glass–ceramics, controlled crystallization plays the key role to engineer the different physico-chemical properties, including thermal expansion characteristics. During controlled heat treatment, large number of tiny nuclei are formed, which lead to growth of different crystalline phases in glass matrix. Li_2O–ZnO–SiO_2 is an interesting system not only because it can be prepared with a wide range of thermal expansion coefficients (from 50 to 200×10^{-7} °C^{-1}) by controlling heat treatments but also because of other growth-related issues [1–4]. This glass–ceramics system does offer a number of distinct advantages over other glass–ceramics, including excellent glass forming ability over a wide range of composition, moderate sealing temperature (less than 1000 °C) coupled with high fluidity and excellent wetting characteristics. They also have high electrical resistivity and good chemical durability. These properties coupled with wide range of TEC make this glass–ceramics material suitable for fabrication of hermetic seals to a variety of metals and alloys including copper, stainless steel, etc. [5–7]. A number of studies on crystallization behaviour and other thermo-physical properties in Li_2O–ZnO–SiO_2 glass–ceramics system have been carried out [8–13]. Cramer von Clausbruch et al. [9] have studied the effect of P_2O_5 on crystallization and microstructure of glass–ceramics in the SiO_2–Li_2O–ZnO–P_2O_5

* Corresponding author. Fax: +91 22 25505151.
E-mail address: gpkoth@apsara.barc.ernet.in (G.P. Kothiyal).

0272-8842/$32.00
doi:10.1016/j.ceramint.2006.01.013

system. They reported that phase transformations and crystallization of lithium disilicate during heating were mainly effected by P_2O_5 content in the samples. In a paper by Donald et al. [13], they have studied the crystallization kinetics with regard to transition metal oxides and have discussed the thermal properties of LZS glass–ceramics related to the microstructure.

In view of designing the LZS material suitable for sealing applications it is very important to monitor the changes in thermal expansion with heat treatment parameters in a fully simulated sealing cycle. With this focus in mind the present studies pertaining to crystallization behaviour of Li_2O–ZnO–SiO_2 system, following two different heating schedules, were carried out. For this we have chosen two different compositions: (a) LZSL composition (wt.%): Li_2O, 12.65; ZnO, 1.85; SiO_2, 74.4; Al_2O_3, 3.8; K_2O, 2.95; P_2O_5, 3.15; and B_2O_3, 1.2 (low ZnO); and (b) LZSH composition (wt.%): Li_2O, 8.9; ZnO, 24.03; SiO_2, 53.7; Na_2O, 5.42; P_2O_5, 2.95; and B_2O_3, 5.0 (high ZnO). Crystallization was carried out in a simulated sealing cycle using both cooling schedule (CS) and heating schedule (HS) for both the compositions and their effects on thermal characteristics and crystalline phases were studied. Significant differences in the formation of crystalline phases and their relative concentrations under two different heating schedules were observed. Finally, hermetic glass–ceramics-to-metal seals were prepared with Cu as well as SS-321 as a demonstration of suitability of material and also studied the interface microstructure to understand the mechanism of sealing using EPMA.

2. Experimental

Two different lithium zinc silicate glasses (a) LZSL and (b) LZSH of nominal compositions (wt.%) as mentioned earlier, were prepared by usual melt and quenched technique. Analytical grade reagents Li_2CO_3, KNO_3, H_3BO_3, ZnO and $(NH_4)_2HPO_4$ were used as starting materials. The batch was subjected to calcination at maximum 850 °C in a predetermined heating schedule using an electrical resistance-heating furnace. The calcination was repeated two to three times after thorough mixing and grinding each time to ensure the uniform composition. The charge was melted in a covered Pt-10% Rh crucible at the temperature about 1450 °C in a raising and lowering hearth furnace (Model OKAY 70R10, M/s BYSAK, Kolkata) and held for 1–2 h for a homogeneous mixing followed by pouring into a pre heated graphite mould. The poured glass was immediately transferred to an annealing furnace set at about 450 °C and held for 2–4 h for annealing before cooling down to room temperature. Clear, transparent and bubble-free glasses were obtained for both the compositions. The details of the experimental procedure are discussed in our earlier paper [8].

A TG-DTA system (Netzsch 409 model) was employed for recording crystallization temperature of the sample. Measurements were done in the temperature range of 30–850 °C employing a heating rate of 10 °C/min. Based on the results of DTA, conversion of glass into glass–ceramics was carried out in a programmable resistance furnace. For this, sample of approximately 12 mm diameter × 6–8 mm height was taken in a graphite crucible and then heated in a protective atmosphere of flowing high purity nitrogen gas. Two different schedules were used for crystallization. In case of heating schedule, the glass sample was first heated up to melting temperature, of about 950 °C and held there for 45 min before cooling down to a temperature about 480 °C at the rate of 5 °C/min. The sample was kept at this temperature for 120 min and then the temperature was increased to the first crystallization temperature followed by second crystallization temperature and at each temperature the sample was held for 60 min. The temperature was then lowered to 450 °C for annealing followed by cooling down to the room temperature.

In the case of cooling schedule, a reverse crystallization cycle as compared to the HS was followed. First the temperature of the sample was raised to 950 °C. After 45 min of dwell time at melting temperature it was lowered to higher crystallization temperature and then to lower crystallization temperature at the rate of 5 °C/min. Dwell time at both the temperatures was 60 min. After crystallization the sample was cooled down to annealing temperature of 450 °C and held for 120 min for annealing. Finally the sample temperature was decreased to room temperature at the rate of 3 °C/min.

Identification of various crystalline phases in glass–ceramics samples was carried out using powder X-ray diffractometer (Philips, model PW 1710) with Cu Kα as X-ray radiation source. The crystalline phases were identified by matching the peak positions of the intense peaks with PCPDF standard cards (24-0686, 89-1813, 77-1140).

The thermal expansion coefficient measurements were carried out in a thermo mechanical analyzer (TMA 92, SETARAM, France) in the temperature range 30–700 °C using a silica probe. For this measurement, first the chamber was evacuated up to 10^{-2} mbar and then flushed with high-purity Ar gas. The measurements were carried out in an inert atmosphere using high-purity Ar (IOLAR grade) with a constant flow rate of 30–40 l/h. The average TEC was calculated in the temperature range of 30–500 °C.

The interface of LZS glass–ceramic to SS-321 alloy seal was studied for microstructure and various elemental inter diffusion using CAMECA SX 100 EPMA. Lithium fluoride (LiF), penta erithrotol (PET) and tallium acid phthalate (TAP) crystals were used for diffracting X-rays. X-rays analysis was done with 20 kV acceleration voltage and 100 nA beam current.

3. Results and discussion

Figs. 1 and 2 show the DTA curves for LZSL and LZSH samples. The endothermic base line shift at ≈460 °C (as shown in Fig. 1) indicates the glass transition temperature in case of LZSL glass system and the sharp exothermic peaks at the onset values of 580 and 780 °C are two crystallization temperatures for this system. For LZSH samples, the glass transition temperature was observed at ≈440 °C and the two crystallization peaks at 570 and 720 °C (Fig. 2). It is seen that in case of LZSL the glass transition temperature is higher as compared to LZSH, which is due to higher SiO_2 content in LZSL sample.

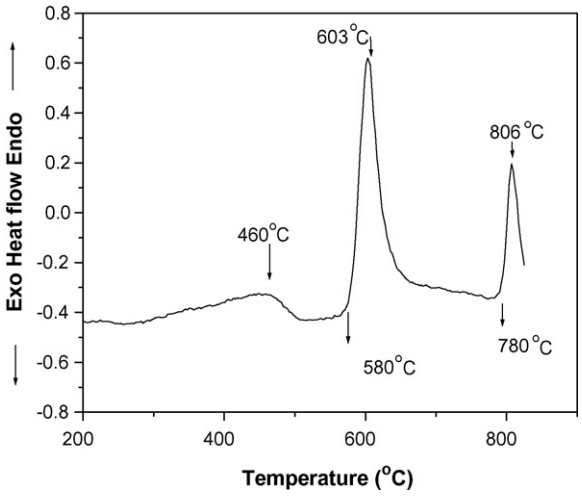

Fig. 1. DTA curve for low zinc LZS (LZSL) glass.

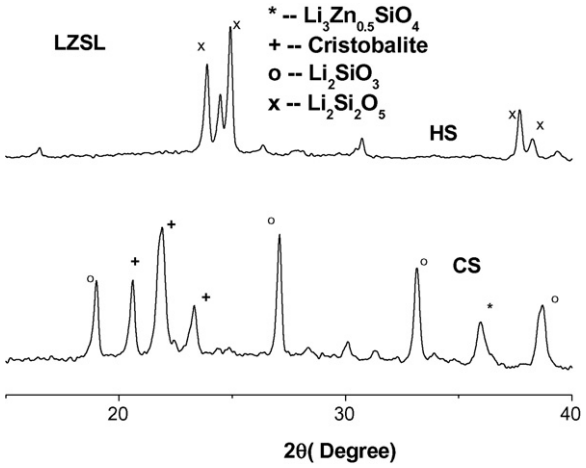

Fig. 3. XRD patterns of the glass–ceramics crystallized with HS and CS for LZSL samples.

Fig. 3 shows the XRD patterns of the LZSL samples crystallized using both heating schedules (CS and HS). These patterns show differences in the formation of crystalline phases and their relative ratios during the two heat treatment processes. Li_2SiO_3 and cristobalite were observed as major crystalline phases during CS. Formation of Li_3PO_4 as separated amorphous phase takes place at high temperature of about 950 °C, which acts as nucleating phase. This promotes the growth of cristobalite when the temperature is lowered to 780 °C and further decreasing the temperature to 580 °C promotes the growth of lithium metasilicate (Li_2SiO_3) with a very small amount of $Li_3Zn_{0.5}SiO_4$ (as sample contains very low ZnO) [8]. This temperature cycle produces the material with the average thermal expansion coefficient value of around 178×10^{-7} °C^{-1}, which matches with the TEC of both Cu metal and SS-321alloy.

In case of HS cycle, few crystallization peaks are observed. The peaks are identified as lithium disilicate ($Li_2Si_2O_5$) in the glass–ceramic sample. During HS, also formation of Li_3PO_4 as separated amorphous phase takes place at high temperature of about 950 °C, which acts as nucleating phase. When heat-treated at 580 °C, it promotes the growth of crystalline lithium metasilicate $Li_2O{\cdot}SiO_2$ on Li_3PO_4. Further increase of the temperature to 780 °C resulted in the growth of lithium disilicate phase. At this temperature, lithium metasilicate and cristobalite react together to form $Li_2O{\cdot}2SiO_2$ ($Li_2Si_2O_5$) as major crystalline phase [14]. The average thermal expansion coefficient value for this material was found to be lower (114×10^{-7} °C^{-1}), primarily due to presence of lithium disilicate major phase having lower thermal expansion coefficient.

The possible mechanism for these is thought to be:

$$3Li_2O + P_2O_5 \rightarrow 2Li_3PO_4 \quad (1)$$

$$Li_2O + SiO_2 \rightarrow Li_2O \cdot SiO_2 \quad (2)$$

$$Li_2O \cdot SiO_2 + SiO_2 \rightarrow Li_2O \cdot 2SiO_2 (Li_2Si_2O_5) \quad (3)$$

Fig. 4 shows the XRD patterns for LZSH sample crystallized using both HS and CS. $Li_3Zn_{0.5}SiO_4$ was identified as major crystalline phase along with some cristobalite phase during HS. In this case, most of $Li_3Zn_{0.5}SiO_4$ phase grew when the sample was heated from nucleating temperature of about 480 °C to lower crystallization temperature of about 600 °C [8]. Later, cristobalite phase is formed at higher crystallization tempera-

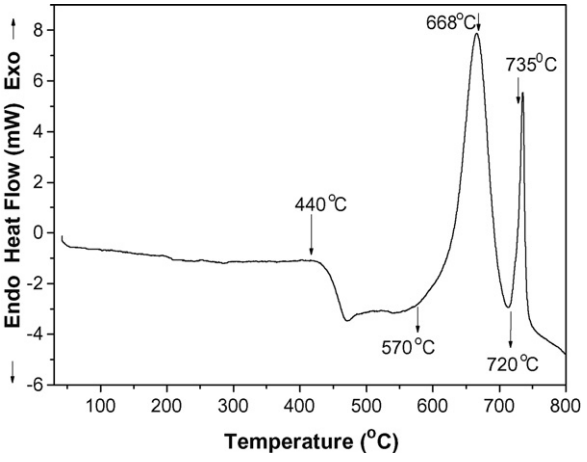

Fig. 2. DTA curve for high zinc LZS (LZSH) glass.

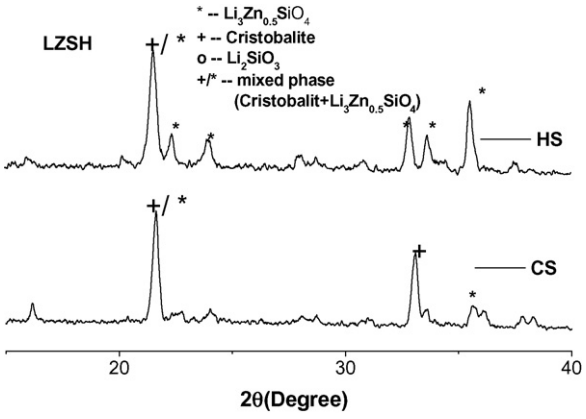

Fig. 4. XRD patterns of the glass–ceramics crystallized with HS and CS for LZSH samples.

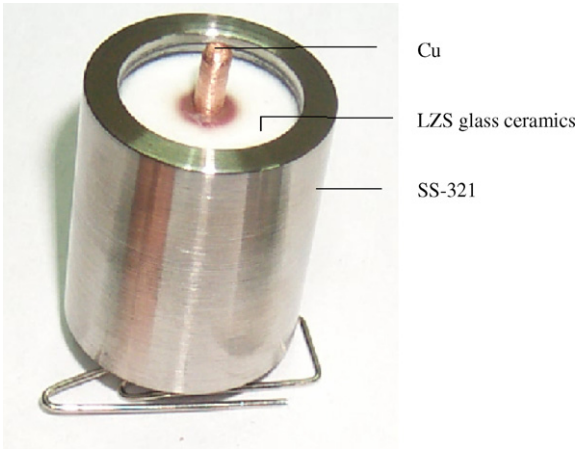

Fig. 5. Photograph of a LZSL glass–ceramics to SS-321 (outer body) hermetic seal.

ture of about 750 °C. When CS was used, it was found that only the outer surface of sample got crystallized in mixed phases of $Li_3Zn_{0.5}SiO_4$ and cristobalite (Fig. 4) leaving the inner portion (bulk) as glass. This inhibits the growth of desired phases/microstructure in the whole material to make it suitable for sealing. However, in the case of HS, the desired crystallization phase/microstructure developed, thereby producing the material with thermal expansion coefficient value of $\approx 185 \times 10^{-7}\ ^{\circ}C^{-1}$ closer to Cu/SS-321.

Fig. 5 shows LZSL glass–ceramic to SS-321 hermetic seal, which withstands a vacuum of 10^{-6} Torr at the helium leak rate of 10^{-9} Torr l/s. Back scattered electron (BSE) image close to the interface for such a seal is shown in Fig. 6a. Globally two different phases represented by bright and dark crystallites are observed in the glass matrix. The dark crystallite is seen to be rich in Si and bright crystallite is slightly depleted in Si. This supports the XRD results, indicating the formation of different phases. Further, there is a thick layer rich in Cr, which seems to be precipitated at the interface (Fig. 6b). The presence of precipitated Cr is confirmed from electron microprobe line scan, as shown in Fig. 7a. Fig. 7b–d also shows the electron microprobe line scans for Ni, Fe and Si, respectively. They show gradual change in the concentrations of elements across the LZSL glass–ceramic-to-SS-321 interface. At higher

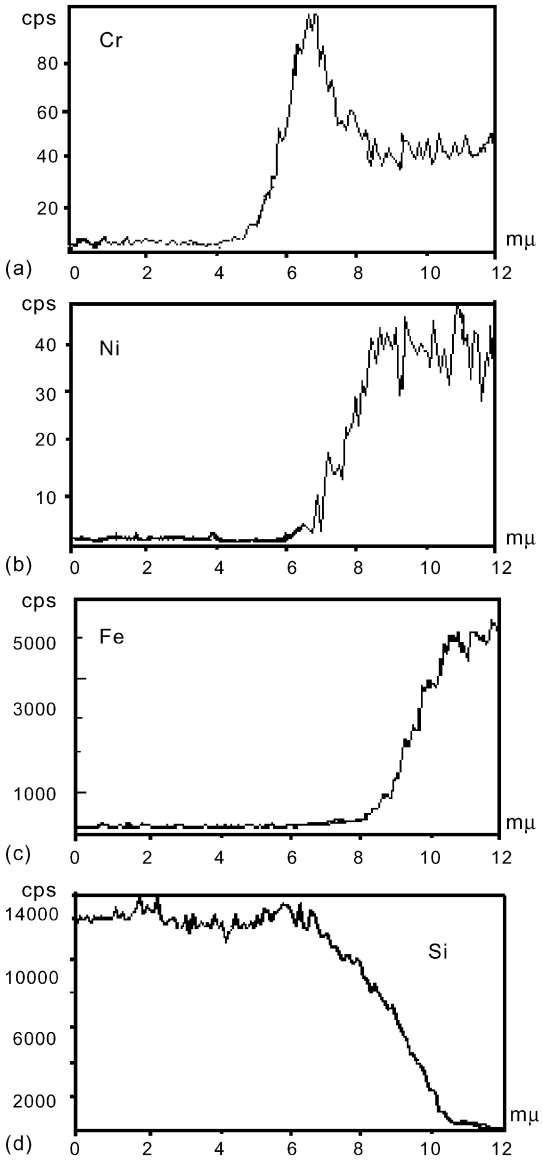

Fig. 7. Electron microprobe line scans across the LZSL glass–ceramic to SS-321 interface. Diffusion and formation of a thick Cr layer (a); diffusion of Ni (b); Fe (c) from SS-321 to LZSL glass–ceramic and diffusion of Si (d) from LZSL glass–ceramic to metal.

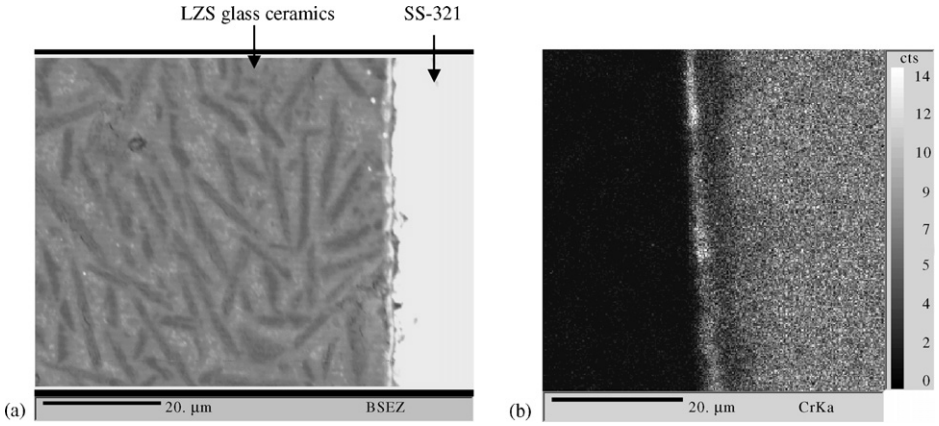

Fig. 6. (a) BSE image for the LZSL glass–ceramic to SS-321 interface and (b) X-rays image at the glass–ceramic/SS-321 metal interface for Cr.

temperature, about 950 °C (sealing temperature) chromium has higher affinity to form oxide layer on the metal surface compared to other elements such as Fe, Ni, etc. present in SS-321 used for fabrication of the seal. As a result, there is a formation of Cr-rich layer at the interface. Si line scan confirmed the diffusion of Si towards the metal region across the Cr-enriched layer and possible formation of Cr_2Si_3 or $LiCr(SiO_3)_2$ at the interface.

The possible reactions for formation of Cr_2O_3 are [4]

$$Cr + Na_2O \rightarrow CrO + 2Na\uparrow \quad (4)$$

$$2CrO + Na_2O \rightarrow Cr_2O_3 + 2Na\uparrow, \text{ or } 3ZnO + 2Cr \rightarrow Cr_2O_3 + 3Zn\uparrow \quad (5)$$

$$Cr_2O_3 + Li_2O(\text{glass}) \rightarrow 2LiCr(SiO_3)_2(\text{precipitated}) \quad (6)$$

The stability and low mobility of this chromium-rich phase creates a potential rather than a gradient at the interface. The presence of this layer slows down the diffusion of Ni and Fe (Fig. 7b and c). Therefore, strong adhesion between the glass–ceramic and SS-321 is promoted by the elemental inter diffusion, primarily of Cr and Si across the interface and formation of a thick layer rich in Cr at the interface.

4. Conclusions

In conclusion, LZSL and LZSH glass–ceramics were prepared. For LZSL the major crystalline phases are Li_2SiO_3 and cristobalite, while for LZSH, $Li_3Zn_{0.5}SiO_4$ and cristobalite are identified as major crystalline phases. The ratio of different crystalline phases is significantly different and mainly depends upon the heating schedule used for crystallization. In case of LZSL, average thermal expansion coefficient values of 178×10^{-7} and 114×10^{-7} °C^{-1} for CS and HS, respectively, are obtained. For LZSH, the average thermal expansion was found to be $\sim 185 \times 10^{-7}$ °C^{-1} in HS, while in CS desired crystalline phase assemblage is inhibited. The TEC of the glass–ceramics LSZL using CS and for LZSH using HS were found to match the TEC of Copper and SS-321. Hermetic seals withstanding a vacuum of 10^{-6} Torr at leak rate 10^{-9} Torr l/s were fabricated with both copper as well as SS-321. Interdiffusion of Cr, Fe, Ni and Si at the interface in the case of LZSL glass–ceramic to SS-321 seals promotes strong adhesion between glass–ceramics and metal. Detailed study of microstructure and crystallite sizes would throw more light on the factors influencing TEC in a more decisive manner.

Acknowledgements

The authors would like to thank Drs V.C. Sahni and J.V. Yakhmi for encouragement and support to this work. They would like to thank Dr N.M. Gupta, Dr G.B. Kale and Dr P.V. Ravindran for providing XRD, EPMA and DTA facilities, respectively. Technical assistance received from Mr B.B. Sawant, Mr A. Sarkar and Mrs Shobha Manikandan is gratefully acknowledged.

References

[1] P.W. Macmillan, G. Patridge, Br. Pat. 943 599, 1963.
[2] R. Morell, K.H.G. Ashbee, High temperature creep of lithium zinc silicate glass–ceramics. Part I. General behaviour and creep mechanism, J. Mater. Sci. 8 (1973) 1253–1270.
[3] R. Morell, K.H.G. Ashbee, High temperature creep of lithium zinc silicate glass–ceramics. Part 2. Compression creep recovery, J. Mater. Sci. 8 (1973) 1271–1277.
[4] I.W. Donald, B.L. Metcalfe, D.J. Wood, J.R. Copley, The preparation and properties of some lithium zinc silicate glass–ceramics, J. Mater. Sci. 24 (1989) 3892–3903.
[5] B.L. Metacalfe, I.W. Donald, Symposium on Glass in Electronics, Society of Glass Technology, Black Pool, 1989.
[6] B.L. Metacalfe, I.W. Donald, in: Proceedings of the Conference Series on the International Conference on New Materials and Their Applications, IOP, Bristol, vol. 111, 1990, pp. 469–478.
[7] B.I. Sharma, M. Goswami, P. Sengupta, V.K. Shrikhande, G.B. Kale, G.P. Kothiyal, Study on some thermo physical properties in Li_2O–ZnO–SiO_2 glass–ceramics, Mater. Lett. 58 (2004) 2423–2428.
[8] I.W. Donald, Preparation, properties and chemistry of glass and glass–ceramics-to-metal seals and coatings, J. Mater. Sci. 28 (1993) 2841–2886.
[9] S. Cramer von Clausbruch, M. Schweiger, W. Höland, V. Rheinberger, The effect of P_2O_5 on crystallization and microstructure of glass–ceramics in Li_2O–SiO_2–K_2O–ZnO–P_2O_5 system, J. Non-Cryst. Solids 263, 264 (2002) 388–394.
[10] A.R. West, F.P. Glasser, Crystallization of lithium zinc silicates. Part I. Phase equillibria in the system Li_4SiO_4–$ZnSiO_4$, J. Mater. Sci. 5 (1970) 557–565.
[11] A.R. West, F.P. Glasser, Crystallization of lithium zinc silicates. Part 2. Comparison of the metastable and stable phase relations and the properties of the lithium zinc orthosilicates, J. Mater. Sci. 5 (1970) 676–688.
[12] Z.X. Chen, P.W. McMillan, Crystallization behaviour of a high zinc content Li_2O–ZnO–SiO_2 glass–ceramics and the effect of K_2O additions, J. Am. Ceram. Soc. 68 (4) (1985) 220–224.
[13] I.W. Donald, B.L. Metcalfe, A.E.P. Morris, Influence of transition metal oxide additions on the crystallization kinetics, microstructures and thermal expansion characteristics of a lithium zinc silicate glass, Mater. Sci. 27 (1992) 2979–2999.
[14] W. Holand, G. Beall, Glass Ceramic Technology, Westerville, 2000.